

B-meson decay constants from improved lattice NRQCD and physical u , d , s and c sea quarks

R. J. Dowdall,^{1,2,*} C. T. H. Davies,^{2,†} R. R. Horgan,¹ C. J. Monahan,³ and J. Shigemitsu⁴
(HPQCD collaboration)[‡]

¹*DAMTP, University of Cambridge, Wilberforce Road, Cambridge CB3 0WA, UK*

²*SUPA, School of Physics and Astronomy, University of Glasgow, Glasgow, G12 8QQ, UK*

³*Physics Department, College of William and Mary, Williamsburg, Virginia 23187, USA*

⁴*Physics Department, The Ohio State University, Columbus, Ohio 43210, USA*

(Dated: November 3, 2018)

We present the first lattice QCD calculation of the decay constants f_B and f_{B_s} with physical light quark masses. We use configurations generated by the MILC collaboration including the effect of u , d , s and c HISQ sea quarks at three lattice spacings and with three u/d quark mass values going down to the physical value. We use improved NRQCD for the valence b quarks. Our results are $f_B = 0.186(4)$ GeV, $f_{B_s} = 0.224(5)$ GeV, $f_{B_s}/f_B = 1.205(7)$ and $M_{B_s} - M_B = 85(2)$ MeV, superseding earlier results with NRQCD b quarks. We discuss the implications of our results for the Standard Model rates for $B_{(s)} \rightarrow \mu^+ \mu^-$ and $B \rightarrow \tau \nu$.

I. INTRODUCTION

The B and B_s decay constants are key hadronic parameters in the Standard Model (SM) rate for $B_{(s)} \rightarrow \mu^+ \mu^-$ and B/B_s oscillations, with the B meson decay constant also determining the rate for $B \rightarrow \tau \nu$. The combination of experiment and theory for these processes provides important constraints on CKM unitarity [1] and the search for new physics, but the strength of the constraints is typically limited by the errors on the hadronic parameters.

The decay constants can only be determined accurately from lattice QCD calculations. Several methods have been developed for this [2], with errors decreasing over the years as calculations have improved. Here we provide a step change in this process, giving the first results for f_B and f_{B_s} that include physical u/d quark masses, obviating the need for a chiral extrapolation. As a result of this and other improvements described below, we have significantly improved accuracy on f_{B_s}/f_B over previous calculations. The implications of our result are discussed in the Conclusions.

II. LATTICE CALCULATION

We use eight ensembles of ‘second-generation’ gluon field configurations recently generated by the MILC collaboration [4, 5], with $N_f = 2 + 1 + 1$ Highly Improved Staggered Quarks (HISQ) [6] in the sea. To control discretisation effects, we use three lattice spacings ranging from 0.15 fm to 0.09 fm and light to strange mass ratios of $m_l/m_s \sim 0.2, 0.1, 0.037$. Details of the ensembles are

TABLE I: Details of the gauge ensembles used in this calculation. β is the gauge coupling, a_Υ is the lattice spacing as determined by the $\Upsilon(2S - 1S)$ splitting in [3], where the three errors are statistics, NRQCD systematics and experiment. am_l, am_s and am_c are the sea quark masses, $L \times T$ gives the spatial and temporal extent of the lattices and n_{cfg} is the number of configurations in each ensemble. The ensembles 1,2 and 3 will be referred to as “very coarse”, 4,5 and 6 as “coarse” and 7,8 as “fine”.

Set	β	a_Υ (fm)	am_l	am_s	am_c	$L \times T$	n_{cfg}
1	5.8	0.1474(5)(14)(2)	0.013	0.065	0.838	16×48	1020
2	5.8	0.1463(3)(14)(2)	0.0064	0.064	0.828	24×48	1000
3	5.8	0.1450(3)(14)(2)	0.00235	0.0647	0.831	32×48	1000
4	6.0	0.1219(2)(9)(2)	0.0102	0.0509	0.635	24×64	1052
5	6.0	0.1195(3)(9)(2)	0.00507	0.0507	0.628	32×64	1000
6	6.0	0.1189(2)(9)(2)	0.00184	0.0507	0.628	48×64	1000
7	6.3	0.0884(3)(5)(1)	0.0074	0.037	0.440	32×96	1008
8	6.3	0.0873(2)(5)(1)	0.0012	0.0363	0.432	64×96	621

shown in table I. The lattice spacings of five of the ensembles were determined using the $\Upsilon(2S - 1S)$ splitting in [3] where details, including a discussion of the systematic errors, can be found. The lattice spacing values of the additional ensembles (sets 3, 6 and 8) are determined in the same way. The valence part of the calculation uses lattice NonRelativistic QCD (NRQCD) [7–9] for the b quarks; the action is described in detail in [3]. It includes a number of improvements over earlier calculations, in particular one-loop radiative corrections (beyond tadpole-improvement) to most of the coefficients of the $\mathcal{O}(v_b^4)$ relativistic correction terms. This action has been shown to give excellent agreement with experiment in recent calculations of the bottomonium [3, 10] and B -meson spectrum [11]. We are now building on previous calculations with the tree level NRQCD action [12–14] to extend this to B -meson decay constants. The b quark mass is tuned, giving the values in Table II, by fixing the spin-averaged kinetic mass with the Υ/η_b masses.

*R.J.Dowdall@damtp.cam.ac.uk

†Christine.Davies@glasgow.ac.uk

‡URL: <http://www.physics.gla.ac.uk/HPQCD>

TABLE II: Parameters used for the valence quarks. am_b is the bare b quark mass in lattice units, u_{0L} is the Landau link value used for tadpole-improvement, and am_l^{val} , am_s^{val} are the HISQ light and strange quark masses.

Set	am_b	u_{0L}	am_l^{val}	am_s^{val}
1	3.297	0.8195	0.013	0.0641
2	3.263	0.82015	0.0064	0.0636
3	3.25	0.819467	0.00235	0.0628
4	2.66	0.834	0.01044	0.0522
5	2.62	0.8349	0.00507	0.0505
6	2.62	0.834083	0.00184	0.0507
7	1.91	0.8525	0.0074	0.0364
8	1.89	0.851805	0.0012	0.0360

The HISQ valence light quark masses are taken to be equal to the sea mass except on set 4 where there is a slight discrepancy. The s quark is tuned using the η_s meson ($M_{\eta_s} = 0.6893(12)$ GeV [3]). Values very close to the sea s masses are found, meaning that partial quenching effects will be small.

To improve the statistical precision of the correlators, we take $U(1)$ random noise sources for the valence quarks using the methods developed in [13]. Along with the point source required for the matrix element, we include gaussian smearing functions for the b quark source with two different widths. We include 16 time sources with b quarks propagating both forward and backward in time on each configuration. We checked the statistical independence of results using a blocked autocorrelation function [3]. Even on the finer physical point ensembles, the correlations are very small between adjacent configurations and the integrated autocorrelation time is consistent with one.

The decay constant is defined from $\langle 0|A_0|B_q\rangle_{\text{QCD}} = M_{B_q} f_{B_q}$, but the quantity that we extract directly from the amplitude of our correlator fits is $\Phi_{B_q} = \sqrt{M_{B_q}} f_{B_q}$; we convert to f_{B_q} at the end. For NRQCD, the full QCD matrix element is constructed from effective theory currents arranged in powers of $1/m_b$. For A_0 we consider the following currents, made from heavy quark Ψ_Q and light quark fields Ψ_q :

$$J_0^{(0)} = \bar{\Psi}_q \gamma_5 \gamma_0 \Psi_Q \quad (1)$$

$$J_0^{(1)} = \frac{-1}{2m_b} \bar{\Psi}_q \gamma_5 \gamma_0 \gamma \cdot \nabla \Psi_Q \quad (2)$$

$$J_0^{(2)} = \frac{-1}{2m_b} \bar{\Psi}_q \gamma \cdot \overleftarrow{\nabla} \gamma_5 \gamma_0 \Psi_Q. \quad (3)$$

These currents are related to the full QCD current through $\mathcal{O}(\alpha_s, \alpha_s \Lambda_{\text{QCD}}/m_b)$ by

$$\langle A_0 \rangle = (1 + \alpha_s z_0) \langle J_0^{(0)} \rangle + (1 + \alpha_s z_1) \langle J_0^{(1)} \rangle + \alpha_s z_2 \langle J_0^{(2)} \rangle \quad (4)$$

One-loop coefficients were calculated in [15]. Here we re-order the perturbation series to make the process of

TABLE III: Coefficients for the perturbative matching of the axial vector current (Eq. 4). $z_0 = \rho_0 - \zeta_{10}$, $z_1 = \rho_1 - z_0$, $z_2 = \rho_2$ from [15].

Set	z_0	z_1	z_2
1	0.024(2)	0.024(3)	-1.108(4)
2	0.022(2)	0.024(3)	-1.083(4)
3	0.022(1)	0.024(2)	-1.074(4)
4	0.006(2)	0.007(3)	-0.698(4)
5	0.001(2)	0.007(3)	-0.690(4)
6	0.001(2)	0.007(2)	-0.690(4)
7	-0.007(2)	-0.031(4)	-0.325(4)
8	-0.007(2)	-0.031(4)	-0.318(4)

TABLE IV: Raw lattice amplitudes for B_s and B from each ensemble, errors are from statistics/fitting only. $a^{3/2}\Phi_q^{(0)}$ and $a^{3/2}\Phi_q^{(1)}$ are the leading amplitude and $1/m_b$ correction.

Set	$a^{3/2}\Phi_s^{(0)}$	$a^{3/2}\Phi_s^{(1)}$	$a^{3/2}\Phi^{(0)}$	$a^{3/2}\Phi^{(1)}$
1	0.3720(10)	-0.0300(3)	0.3220(19)	-0.0260(3)
2	0.3644(6)	-0.0291(3)	0.3093(11)	-0.0257(8)
3	0.3621(16)	-0.0288(2)	0.2986(17)	-0.0237(4)
4	0.2733(4)	-0.0234(2)	0.2373(9)	-0.0197(4)
5	0.2679(3)	-0.0234(1)	0.2272(7)	-0.0197(3)
6	0.2653(2)	-0.0229(1)	0.2193(8)	-0.0194(3)
7	0.1747(3)	-0.0170(1)	0.1525(8)	-0.0146(6)
8	0.1694(3)	-0.0167(0)	0.1386(5)	-0.0136(1)

renormalisation clearer. The z_i depend on am_b and are given in Table III for the range of masses needed here. We see that the one-loop renormalisation of the tree-level current, $J_0^{(0)} + J_0^{(1)}$, is tiny [31]. z_0 includes the effect of mixing between $J_0^{(0)}$ and $J_1^{(1)}$ at one-loop. We evaluate the renormalisation of Eq. 4 using α_s in the V-scheme at scale $q = 2/a$. Values for α_s are obtained by running down from $\alpha_s^{\overline{\text{MS}}}(M_Z) = 0.1184$ [16] and range from 0.285 to 0.314.

III. RESULTS

We fit heavy-light meson correlators with both $J_0^{(0)}$ and $J_0^{(1)}$ operators at the sink simultaneously using a multi-exponential Bayesian fitting procedure [17]. The

TABLE V: Raw lattice energies from each ensemble, errors are from statistics/fitting only. aM_π are the pion masses used in the chiral fits, $aE(B_s)$ and $aE(B)$ are the energies of the B_s and B meson. Results on sets 3, 6 and 8 are new, others are given in [11].

Set	aM_π	$aE(B_s)$	$aE(B)$
3	0.10171(4)	0.6067(7)	0.5439(12)
6	0.08154(2)	0.5158(1)	0.4649(6)
8	0.05718(1)	0.4025(2)	0.3638(5)

B and B_s are fit separately; priors used in the fit are described in [11]. The amplitudes and energies from the fits are given in Tables IV and V. $a^{3/2}\Phi_q^{(0)}$ is the matrix element of the leading current $J_0^{(0)}$ and $a^{3/2}\Phi_q^{(1)}$ that of $J_0^{(1)}$ and $J_0^{(2)}$, whose matrix elements are equal at zero meson momentum. Notice that the statistical errors in Φ do not increase on the physical point lattices, because they have such large volumes.

We take two approaches to the analysis. The first is to perform a simultaneous chiral fit to all our results for Φ , Φ_s , Φ_s/Φ and $M_{B_s} - M_B$ using $SU(2)$ chiral perturbation theory. The second is to study only the physical u/d mass results as a function of lattice spacing.

For the chiral analysis we use the same formula and priors for $M_{B_s} - M_B$ as in [11]. Pion masses used in the fits are listed in Table V and the chiral logarithms, $l(M_\pi^2)$, include the finite volume corrections computed in [18] which have negligible effect on the fit. For the decay constants the chiral formulas, including analytic terms up to M_π^2 and the leading logarithmic behaviour, are (see e.g. [19]):

$$\Phi_s = \Phi_{s0}(1.0 + b_s M_\pi^2/\Lambda_\chi^2) \quad (5)$$

$$\Phi = \Phi_0 \left(1.0 + b_l \frac{M_\pi^2}{\Lambda_\chi^2} + \frac{1 + 3g^2}{2\Lambda_\chi^2} \left(-\frac{3}{2} l(M_\pi^2) \right) \right) \quad (6)$$

The coefficients of the analytic terms b_s, b_l are given priors 0.0(1.0) and Φ_0, Φ_{s0} have 0.5(5). To allow for discretisation errors each fit formula is multiplied by $(1.0 + d_1(\Lambda a)^2 + d_2(\Lambda a)^4)$, with $\Lambda = 0.4$ GeV. We expect discretisation effects to be very similar for Φ and Φ_s and so we take the d_i to be the same, but differing from the d_i used in the $M_{B_s} - M_B$ fit. Since all actions used here are accurate through a^2 at tree-level, the prior on d_1 is taken to be 0.0(3) whereas d_2 is 0.0(1.0). The d_i are allowed to have mild m_b dependence as in [11]. The ratio Φ_s/Φ is allowed additional light quark mass dependent discretisation errors that could arise, for example, from staggered taste-splittings.

Error %	Φ_{B_s}/Φ_B	$M_{B_s} - M_B$	Φ_{B_s}	Φ_B
EM:	0.0	1.2	0.0	0.0
a dependence:	0.01	0.9	0.7	0.7
chiral:	0.01	0.2	0.05	0.05
g :	0.01	0.1	0.0	0.0
stat/scale:	0.30	1.2	1.1	1.1
operator:	0.0	0.0	1.4	1.4
relativistic:	0.5	0.5	1.0	1.0
total:	0.6	2.0	2.0	2.1

TABLE VI: Full error budget from the chiral fit as a percentage of the final answer.

The results of the decay constant chiral fits are plotted in Figs. 1 and 2. Extrapolating to the physical point appropriate to $m_l = (m_u + m_d)/2$ in the absence of electromagnetism, i.e. $M_\pi = M_{\pi^0}$, we find $\Phi_{B_s} =$

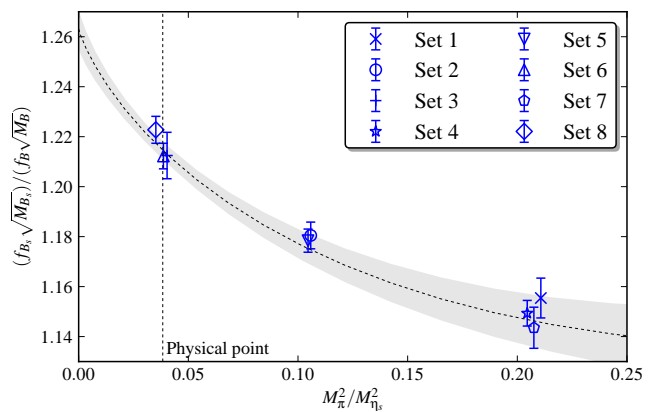


FIG. 1: Fit to the decay constant ratio Φ_{B_s}/Φ_B . The fit result is shown in grey and errors include statistics, and chiral/continuum fitting.

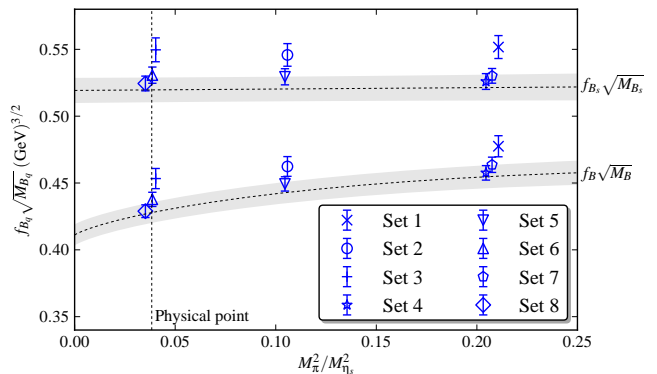


FIG. 2: Fit to the decay constants Φ_{B_s} and Φ_B . Errors on the data points include statistics/scale only. The fit error, in grey, includes chiral/continuum fitting and perturbative errors.

$0.520(11)$ GeV $^{3/2}$, $\Phi_B = 0.428(9)$ GeV $^{3/2}$, $\Phi_{B_s}/\Phi_B = 1.215(7)$. For $M_{B_s} - M_B$ we obtain 86(1) MeV, in agreement with the result of [11].

Figs 3 and 4 show the results of fitting $M_{B_s} - M_B$ and decay constants from the physical point ensembles only, and allowing only the mass dependent discretisation terms above. The results are $\Phi_{B_s} = 0.515(8)$ GeV $^{3/2}$, $\Phi_B = 0.424(7)$ GeV $^{3/2}$, $\Phi_{B_s}/\Phi_B = 1.216(7)$ and $M_{B_s} - M_B = 87(1)$ MeV. Results and errors agree well between the two methods and we take the central values from the chiral fit as this allows us to interpolate to the correct pion mass.

Our error budget is given in Table VI. The errors that are estimated directly from the chiral/continuum fit are those from statistics, the lattice spacing and g and other chiral fit parameters. The two remaining sources of error in the decay constant are missing higher order corrections in the operator matching and relativistic corrections to the current. We estimate the operator matching error by allowing in our fits for an am_b -dependent α_s^2 correction to the renormalisation in Eq. 4 with prior on the coefficient

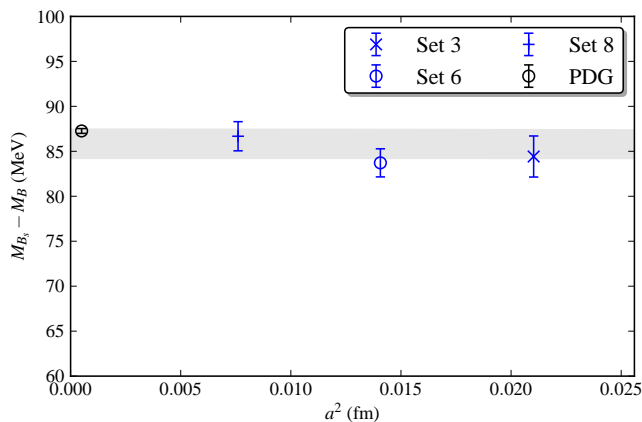


FIG. 3: Fit to the mass difference $M_{B_s} - M_B$ on the three physical point ensembles only. Errors on data points include statistics and scale, the fit error is shown in grey. An electromagnetic correction of $-1(1)$ MeV has been applied to the lattice results and the fit to allow comparison with experiment.

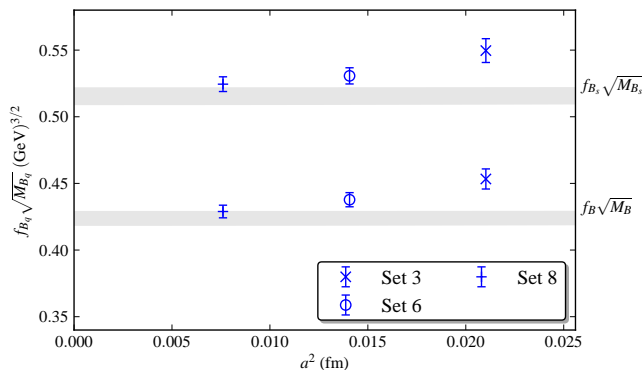


FIG. 4: Fit to the decay constants Φ_{B_s} and Φ_B on the three physical point ensembles only. Errors on the data points include statistics/scale only. The fit error includes chiral/continuum fitting and perturbative errors.

of $0.0(2)$ i.e. ten times the size of the one-loop correction, z_0 . This error cancels in the ratio f_{B_s}/f_B . We also allow for α_s^2 corrections multiplying $J_0^{(1,2)}$ with coefficient $0.0(1.0)$. The matrix element of $J_0^{(1)}$ is about 10% of $J_0^{(0)}$ from Table IV. Missing current corrections at the next order in $1/m_b$ will be of size $(\Lambda_{\text{QCD}}/m_b)^2 \simeq 0.01$ which we take as an error. Finally, we estimated in [11] that to correct for missing electromagnetic effects, $M_{B_s} - M_B$ should be shifted by $-1(1)$ MeV.

Using the PDG masses $M_{B_i} = (M_{B^0} + M_{B^\pm})/2 = 5.27942(12)$ GeV and $M_{B_s} = 5.36668(24)$ GeV [20] to convert Φ_q to f_{B_q} our final results are:

$$\begin{aligned} f_B &= 0.186(4) \text{ GeV} \\ f_{B_s} &= 0.224(5) \text{ GeV} \\ f_{B_s}/f_B &= 1.205(7) \\ M_{B_s} - M_B &= 85(2) \text{ MeV.} \end{aligned} \quad (7)$$

For the B meson decay constant we need to distinguish between f_{B_d} and f_{B_u} . Since sea quark mass effects are much smaller than valence mass effects we simply do this by extrapolating Φ_{B_s} and Φ_B to values of M_π^2 corresponding to fictitious mesons made purely of u or d quarks using $m_u/m_d = 0.48(10)$ [20]. This gives:

$$\begin{aligned} f_{B_s}/f_{B^+} &= 1.217(8) ; f_{B_s}/f_{B^0} = 1.194(7) \\ f_{B^+} &= 0.184(4) \text{ GeV} ; f_{B^0} = 0.188(4) \text{ GeV} \end{aligned} \quad (8)$$

IV. CONCLUSIONS

Our results agree with but improve substantially on two earlier results using nonrelativistic approaches for the b quark and multiple lattice spacing values on $N_f = 2+1$ ensembles using asqtad sea quarks. These were: $f_{B_s} = 228(10)$ MeV, $f_{B_s}/f_B = 1.188(18)$ (NRQCD/HISQ) [14] and $f_{B_s} = 242.0(9.5)$ MeV and $f_{B_s}/f_{B^+} = 1.229(26)$ (Fermilab/asqtad) [21]. We also agree well (within the 2% errors) with a previous result for f_{B_s} of 225(4) MeV obtained using a relativistic (HISQ) approach to b quarks on very fine $N_f = 2+1$ lattices [22]. Our simultaneous determination of $M_{B_s} - M_B$ to 2% agrees with experiment (87.4(3) MeV [20]).

We can determine new lattice ‘world-average’ error-weighted values by combining our results in Eq. 7 with the independent results of [21] and [22] since effects from c sea quarks, which they do not include, should be negligible [23]. The world averages are then: $f_{B_s} = 225(3)$ MeV and $f_{B_s}/f_{B^+} = 1.218(8)$ giving $f_{B^+} = 185(3)$ MeV.

These allow for significant improvements in predictions for SM rates. For example, updating [24] with the world-average for f_{B_s} above and our result for f_{B^0} (Eq. 8) we obtain:

$$\begin{aligned} \text{Br}(B_s \rightarrow \mu^+ \mu^-) &= 3.17 \pm 0.15 \pm 0.09 \times 10^{-9} \\ \text{Br}(B_d \rightarrow \mu^+ \mu^-) &= 1.05 \pm 0.05 \pm 0.05 \times 10^{-10} \end{aligned} \quad (9)$$

where the second error from f_{B_q} has been halved and is no longer larger than other sources of error such as $V_{tb}^* V_{tq}$. Note that this is the flavor-averaged branching fraction at $t = 0$; the time-integrated result would be increased by 10% in the B_s case (to $3.47(19) \times 10^{-9}$) to allow for the width difference of the two eigenstates [25, 26]. The current experimental results [27] for $B_s \rightarrow \mu^+ \mu^-$ agree with this prediction.

From the world-average f_{B^+} above we also obtain the Standard Model rate:

$$\frac{1}{|V_{ub}|^2} \text{Br}(B^+ \rightarrow \tau \nu) = 6.05(20), \quad (10)$$

with 3% accuracy. Calculations of matrix elements for B_s/B mixing with physical u/d quarks are now underway.

Acknowledgements We are grateful to the MILC collaboration for the use of their gauge configurations and to B. Chakraborty, J. Koponen and P. Lepage for useful

discussions. The results described here were obtained using the Darwin Supercomputer of the University of Cambridge High Performance Computing Service as part of

STFC's DiRAC facility. This work was funded by STFC and the US DOE.

-
- [1] J. Laiho, E. Lunghi, and R. Van de Water, PoS **LATTICE2011**, 018 (2011), 1204.0791.
- [2] C. Davies, PoS **LATTICE2011**, 019 (2011), 1203.3862.
- [3] R. Dowdall et al. (HPQCD Collaboration), Phys.Rev. **D85**, 054509 (2012), 1110.6887.
- [4] A. Bazavov et al. (MILC), Phys.Rev. **D82**, 074501 (2010), 1004.0342.
- [5] M. collaboration (MILC Collaboration) (2012), 1212.4768.
- [6] E. Follana et al. (HPQCD Collaboration), Phys.Rev. **D75**, 054502 (2007), hep-lat/0610092.
- [7] G. Lepage, L. Magnea, C. Nakhleh, U. Magnea, and K. Hornbostel, Phys.Rev. **D46**, 4052 (1992), hep-lat/9205007.
- [8] B. Thacker and G. Lepage, Phys.Rev. **D43**, 196 (1991).
- [9] A. Gray, I. Allison, C. Davies, E. Dalgic, G. Lepage, et al. (HPQCD Collaboration), Phys.Rev. **D72**, 094507 (2005), hep-lat/0507013.
- [10] J. Daldrop, C. Davies, and R. Dowdall (HPQCD Collaboration), Phys.Rev.Lett. **108**, 102003 (2012), 1112.2590.
- [11] R. Dowdall, C. Davies, T. Hammant, and R. Horgan, Phys.Rev. **D86**, 094510 (2012), 1207.5149.
- [12] E. Gamiz, C. T. Davies, G. P. Lepage, J. Shigemitsu, and M. Wingate (HPQCD Collaboration), Phys.Rev. **D80**, 014503 (2009), 0902.1815.
- [13] E. B. Gregory et al. (HPQCD Collaboration), Phys. Rev. **D83**, 014506 (2011), 1010.3848.
- [14] H. Na, C. J. Monahan, C. T. Davies, R. Horgan, G. P. Lepage, et al., Phys.Rev. **D86**, 034506 (2012), 1202.4914.
- [15] C. Monahan, J. Shigemitsu, and R. Horgan (2012), 1211.6966.
- [16] C. McNeile, C. T. H. Davies, E. Follana, K. Hornbostel, and G. P. Lepage (HPQCD Collaboration), Phys. Rev. **D82**, 034512 (2010), 1004.4285.
- [17] G. P. Lepage et al., Nucl. Phys. Proc. Suppl. **106**, 12 (2002), hep-lat/0110175.
- [18] C. Bernard (MILC Collaboration), Phys.Rev. **D65**, 054031 (2002), hep-lat/0111051.
- [19] C. Albertus, Y. Aoki, P. Boyle, N. Christ, T. Dumitrescu, et al., Phys.Rev. **D82**, 014505 (2010), 1001.2023.
- [20] J. Beringer et al. (Particle Data Group), Phys. Rev. **D86**, 010001 (2012).
- [21] A. Bazavov et al. (Fermilab Lattice Collaboration, MILC Collaboration), Phys.Rev. **D85**, 114506 (2012), 1112.3051.
- [22] C. McNeile, C. T. H. Davies, E. Follana, K. Hornbostel, and G. P. Lepage (HPQCD Collaboration) (2011), 1110.4510.
- [23] C. Davies, C. McNeile, E. Follana, G. Lepage, et al. (HPQCD Collaboration), Phys.Rev. **D82**, 114504 (2010), 1008.4018.
- [24] A. J. Buras, J. Girrbach, D. Guadagnoli, and G. Isidori, Eur.Phys.J. **C72**, 2172 (2012), 1208.0934.
- [25] K. De Bruyn, R. Fleischer, R. Knegjens, P. Koppenburg, M. Merk, et al., Phys.Rev.Lett. **109**, 041801 (2012), 1204.1737.
- [26] R. Aaij et al., LHCb-CONF-2012-002 (2012).
- [27] R. Aaij et al. (LHCb Collaboration), Phys.Rev.Lett. **110**, 021801 (2013), 1211.2674.
- [28] J. Harada, S. Hashimoto, K.-I. Ishikawa, A. S. Kronfeld, T. Onogi, et al., Phys.Rev. **D65**, 094513 (2002), hep-lat/0112044.
- [29] P. Boyle and C. Davies (UKQCD Collaboration), Phys.Rev. **D62**, 074507 (2000), hep-lat/0003026.
- [30] G. Donald, C. Davies, R. Dowdall, E. Follana, K. Hornbostel, et al., Phys.Rev. **D86**, 094501 (2012), 1208.2855.
- [31] This agrees with expectations from [21, 28] in which the heavy-light renormalisation constant is perturbatively very close to the product of the square roots of the renormalisation of the local temporal vector current for heavy-heavy and light-light. Here the corresponding heavy-heavy current is conserved [29] and the light-light current has a very small renormalisation [30]. This will be discussed further elsewhere.